

# Highly resistive Cu(In,Ga)Se<sub>2</sub> absorbers for improved low-irradiance performance of thin-film solar cells

A. Virtuani<sup>a,\*</sup>, E. Lotter<sup>a</sup>, M. Powalla<sup>a</sup>, U. Rau<sup>b</sup>, J.H. Werner<sup>b</sup>

<sup>a</sup>Zentrum fuer Sonnenenergie- und Wasserstoff- Forschung Baden-Württemberg (ZSW) Industriestr. 6, 70565 Stuttgart, Germany

<sup>b</sup>Institut für Physikalische Elektronik, Universität Stuttgart, Pfaffenwaldring 47, 70569 Stuttgart, Germany

## Abstract

This paper reports on the investigation of Cu(In,Ga)Se<sub>2</sub> thin-film solar cells for application under low irradiance conditions with irradiance  $E < 1$  mW/cm<sup>2</sup>. Under such conditions, a parallel resistance  $R_p > 10$  kΩ cm<sup>2</sup> of the solar cells is required. We find that Cu(In,Ga)Se<sub>2</sub> absorber material with a low Cu content of 18 at.% provides  $R_p > 100$  kΩ cm<sup>2</sup> and enables solar cells to exhibit a power conversion efficiency of 6% under an irradiance  $E = 0.1$  mW/cm<sup>2</sup>. Under such conditions, standard Cu(In,Ga)Se<sub>2</sub> absorber material with a Cu content of 21.5 at.% is not a suitable photovoltaic absorber material because the  $R_p$  of the corresponding solar cells is too low. Further investigations of different solar cells with a variety of Cu contents in the absorber material reveal that the shunt resistance of the solar cells is proportional to the bulk resistivity of the corresponding Cu(In,Ga)Se<sub>2</sub> absorber materials. This observation leads us to the proposition that the parallel resistance in Cu(In,Ga)Se<sub>2</sub> solar cells originates from highly localised shunt regions in the absorber material.

© 2003 Elsevier B.V. All rights reserved.

**Keywords:** Cu(In,Ga)Se<sub>2</sub>; Indoor application; Parallel resistance

## 1. Introduction

The use of solar cells as power generators for consumer electronics requires optimisation of the devices for operation under indoor conditions with irradiances that are much lower than the usual standard test conditions (STC) with an irradiance  $E = 100$  mW/cm<sup>2</sup> (1 sun). Operation of a solar cell under low irradiance requires a high shunt (parallel) resistance  $R_p$  of the device [1,2]. Cu(In,Ga)Se<sub>2</sub> thin-film solar cells usually have  $R_p \approx 10$  kΩ cm<sup>2</sup>, a value which leads to a severe degradation the cell performance for  $E < 1$  mW/cm<sup>2</sup> [3]. The present paper reports on a new approach to realise Cu(In,Ga)Se<sub>2</sub> solar cells with a much higher  $R_p$ . These cells utilise a Cu(In,Ga)Se<sub>2</sub> absorber material with a Cu atomic content of only 18 at.%. The use of this absorber material allows values for  $R_p$  that are more than one order of magnitude higher than for standard cells made from absorbers with a Cu content of 21.5 at.%. The solar cells that use the Cu-poor absorber material are suitable for application in the typical range

of illumination intensities encountered in indoor environments, varying between 0.05 and 5 mW/cm<sup>2</sup>, depending on the light sources, on the distance from the light sources, and on the presence of reflected or diffused light. We observe that the shunt resistance of different solar cells is proportional to the bulk resistivity of the corresponding Cu(In,Ga)Se<sub>2</sub> absorber materials and discuss the physical nature of the parallel resistance  $R_p$  in Cu(In,Ga)Se<sub>2</sub> solar cells.

## 2. Experimental details

A series of Cu(In,Ga)Se<sub>2</sub> films was deposited in an in-line, bilayer process by multiple-source evaporation on soda lime glass and on Mo-coated soda lime glass substrates with a thickness of approximately 2 μm. The copper content in the film was varied in the range  $0.59 \leq [\text{Cu}]/([\text{In}] + [\text{Ga}]) \leq 0.89$ , corresponding to a Cu atomic content between 18 and 23.3 at.%, the relative Se content in the film was kept constant and the  $[\text{Ga}]/[\text{Ga}] + [\text{In}]$  ratio was approximately 0.33. Films grown on glass were then used to measure the resistivity of the absorber material. Cells were realised using films deposited on Mo-coated glass by growing a thin CdS buffer

\*Corresponding author. Tel.: +49-711-7870-234; fax: +49-711-7870-230.

E-mail address: [virtuani@zsw-bw.de](mailto:virtuani@zsw-bw.de) (A. Virtuani).

Table 1

Diode parameters, as extrapolated from the illuminated (100 mW/cm<sup>2</sup>) and dark *JV* curves, of the three cells with different Cu contents (*I*=1sun/*d*=dark)

Sample name	Cu content [at.%]	<i>n</i> ( <i>I</i> / <i>d</i> )	<i>J</i> <sub>0</sub> (A/cm <sup>2</sup> ) ( <i>I</i> / <i>d</i> )	<i>R</i> <sub>s</sub> (Ω cm <sup>2</sup> ) ( <i>I</i> / <i>d</i> )	<i>R</i> <sub>p</sub> (kΩ cm <sup>2</sup> ) ( <i>I</i> / <i>d</i> )
cr	23.3	1.6/1.7	3.6×10 <sup>-9</sup> /4.8×10 <sup>-9</sup>	0.4/0.6	1.9/3.5
std	21.5	1.7/1.9	1.5×10 <sup>-8</sup> /3.1×10 <sup>-8</sup>	0.6/1	1.7/11.8
cp	18	1.5/1.5	8×10 <sup>-10</sup> /1×10 <sup>-9</sup>	0.6/0.8	1.9/142

layer on them by chemical bath deposition, followed by sputtering a double-layer of undoped ZnO and Al-doped ZnO (Al:ZnO) for the window. The solar cells, which have a size of 0.5 cm<sup>2</sup>, were finally completed with an evaporated a Ni/Al front grid on top.

Typical solar cells and modules developed in our laboratories have an atomic copper content of 21.5% ([Cu]/[In] + [Ga] ≅ 0.8) [4]. A Cu content lower than 25 at.% required for the stoichiometric compound is usually taken to avoid the presence of Cu<sub>y</sub>Se segregations which are usually present when depositing the stoichiometric or near-stoichiometric compound on large areas [5]. The actual composition of our films was determined by means of X-ray fluorescence measurements (XRF). Our set-up is ±0.5 at.%, accurate in the determination of the actual atomic content of an element.

The performance of three cells containing a different amount of Cu in the absorber material is characterised under different illumination intensities which were varied by placing wire meshes between the light source and the measured samples. We then compare the low-irradiance performance of the cells with some physical characteristics (resistivity and morphology) of the corresponding absorber material. The resistivity of the films grown on glass was measured with a four-point measurement set-up and their morphology was investigated by scanning electron microscopy (SEM) with a FEI XL-30 SFEG/Sirius microscope.

Solar cells were characterised by means of current density (*J*) vs. voltage (*V*) measurements under a simulated AM 1.5 spectrum. Information from the characteristics was extracted by fitting them to a standard single-diode model

$$J(V) = J_0 \left[ \exp \left( \frac{q(V - JR_s)}{nkT} \right) - 1 \right] - J_{ph} + \frac{V - JR_s}{R_p} \quad (1)$$

where *J*<sub>0</sub> is the reverse saturation current density of the diode, *q* is the electron charge, *n* is the diode ideality factor, *k* is the Boltzmann constant, *T* the absolute temperature and *J*<sub>ph</sub> the photogenerated current. The quantities *R*<sub>s</sub> and *R*<sub>p</sub> denote the series and the parallel parasitic resistances. Fits of the *JV* curves were carried out using a commercially available program (Diploplot [6])

which allows direct fitting of the parameters to the transcendental equation (Eq. (1)).

### 3. Results and discussion

Three solar cells with a different atomic copper content (18, 21.5, and 23.3 at.%) of the absorber material were characterised by varying the irradiance over more than three orders of magnitude, and the diode parameters of the three cells were then extrapolated. In the following we will refer to these three samples as the cp (copper poor), the std (standard) and the cr (copper richer) cell, respectively.

Table 1 shows the values of the diode parameters *J*<sub>0</sub>, *n*, *R*<sub>s</sub>, and *R*<sub>p</sub> obtained from the illuminated (100 mW/cm<sup>2</sup>) and the dark *JV* curves. Comparison of the parameters does not unveil large differences between the dark and light behaviour of the three samples. The ideality factor *n* and the reverse saturation current *J*<sub>0</sub> just slightly increase when moving from the illuminated to the dark characteristics, remaining approximately constant which suggests that the current transport mechanism across the cell junction is not altered when moving from light to dark operation. Both the parasitic resistances tend to increase when moving towards lower irradiances. This behaviour seems to be related to the photoconductivity of the absorber material. The series resistances *R*<sub>s</sub> of the three cells have comparable values and increase just slightly. The shunt resistances *R*<sub>p</sub> of the three cells are similar only under illumination, whereas they differ considerably in the dark. The ratio between the shunt resistance in the dark and that under 1 sun illumination *R*<sub>p</sub>(dark)/*R*<sub>p</sub>(100 mW/cm<sup>2</sup>) is approximately 2, 10, and 100 for the cr, the std, and the cp cell, respectively, implying that the dark *R*<sub>p</sub> of the cp cell (142 kΩ cm<sup>2</sup>) is more than one order of magnitude larger than *R*<sub>p</sub>(dark) of the std cell (11.8 kΩ cm<sup>2</sup>), and 50 times larger than that of the cr cell.

#### 3.1. Irradiance dependence of the efficiency

Fig. 1a–c compares the relationship between the irradiance *E* and the solar cell efficiencies *η*, the open-circuit voltages *V*<sub>OC</sub>, and the fill factors *FF* of the three solar cells discussed above. Under STC the two cells with a higher copper content have an efficiency *η* of

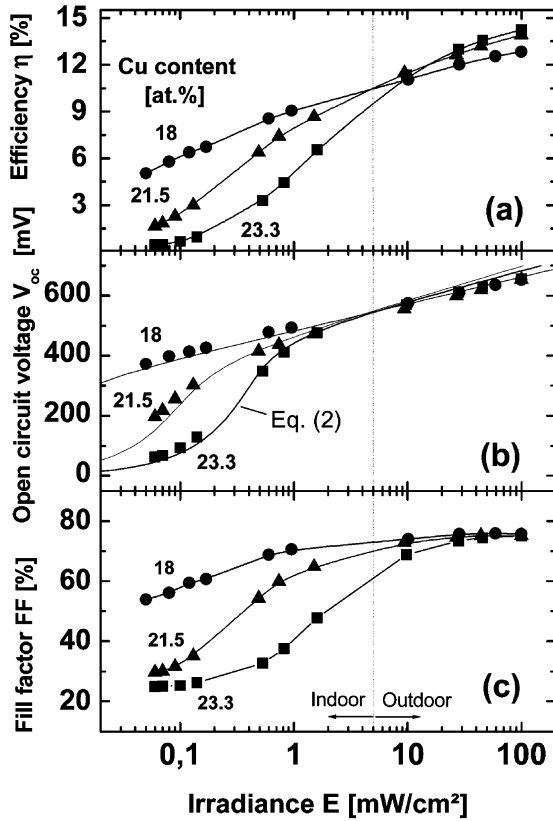


Fig. 1. Irradiance dependence of the efficiency  $\eta$  (a), of the open-circuit voltage  $V_{OC}$  (b), and of the fill factor  $FF$  (c) of the cells realised with different atomic Cu contents of the absorber material. Lines are included as guides to the eye in (a) and (c). In (b) they are curves derived from Eq. (2) using the dark diode parameters presented in Table 1. The typical indoor and outdoor irradiance ranges are also indicated.

approximately 14%. With lower irradiances the decline of efficiency is stronger for the cr cell which retains only  $\eta = 0.7\%$  at  $0.1 \text{ mW}/\text{cm}^2$ , a typical irradiance level encountered indoors. The std cell at this irradiance has an efficiency of approximately 2.5%. The cp cell shows a moderate  $\eta = 12.8\%$  under STC due to a lower value of the short-circuit current  $J_{sc}$ . However, the efficiency decrease when moving towards lower irradiances is much smaller than in the other two cells, retaining  $\eta = 10\%$  at  $5 \text{ mW}/\text{cm}^2$  and  $\eta = 6\%$  at  $0.1 \text{ mW}/\text{cm}^2$ .

The efficiency  $\eta$  is determined by the irradiance dependence of the short-circuit current  $J_{sc}$ , the open-circuit voltage  $V_{OC}$ , and the fill factor  $FF$ . In standard  $\text{Cu}(\text{In,Ga})\text{Se}_2$   $J_{sc}$  is directly proportional to the irradiance  $E$ :  $J_{sc} = \alpha E$ , where  $\alpha$  is a proportionality constant. The decline of efficiency of these cells under low irradiances results from the fact that  $V_{OC}$  and  $FF$  are limited by the low value of  $R_p$  [3]. We will now focus our attention on the irradiance dependence of  $V_{OC}$  and  $FF$  for the three cells under discussion.

### 3.2. Irradiance dependence of the open-circuit voltage

Neglecting the effect of the series resistance ( $R_s \approx 0$ ) and taking  $J_{ph} = J_{sc}$  in Eq. (1) leads to

$$J_{sc} = \alpha E = J_0 \left[ \exp\left(\frac{qV_{OC}}{nkT}\right) - 1 \right] + \frac{V_{OC}}{R_p} \quad (2)$$

which establishes a relationship between the irradiance  $E$  and the  $V_{OC}$  of the cell.

Since  $n$  and  $J_0$  of the three cells do not vary significantly when moving towards lower irradiances, we take the diode parameters of the dark  $JV$  characteristics and insert them into Eq. (2). The simulated  $V_{OC}(E)$  curves are shown in Fig. 1b and are in good agreement with the measured data.

Under STC, the three cells have a comparable  $V_{OC}$  ( $\approx 654 \text{ mV}$ ). Under low irradiances (values lower than  $1 \text{ mW}/\text{cm}^2$ ), however, the values of  $V_{OC}$  of the cr cell and of the std cell, which have smaller  $R_p$ , abruptly decrease (the decrease is lower for the std cell). If  $R_p \approx \infty$  and  $V_{OC} \gg nkT/q$ , it follows from Eq. (2):

$$V_{OC} = \frac{nkT}{q} \ln\left(\frac{J_{sc}}{J_0}\right) = \frac{nkT}{q} [\ln(E) + \ln(\alpha) - \ln(J_0)] \quad (3)$$

We would therefore expect a linear behaviour in a semi-logarithmic plot of  $V_{OC}$  vs. irradiance  $E$ .

Among the devices under investigation only the cp cell ( $R_p > 10^5 \text{ k}\Omega \text{ cm}^2$ ) follows this linear dependence on  $E$  down to the lowest irradiation levels. This cell still retains a  $V_{OC} = 405 \text{ mV}$  at  $0.1 \text{ mW}/\text{cm}^2$ , whereas the  $V_{OC}$  of the other cells at irradiances  $E < 1 \text{ mW}/\text{cm}^2$  is increasingly deteriorated by the low  $R_p$ . Note that  $R_p$  at  $E < 1 \text{ mW}/\text{cm}^2$  almost equals the dark value.

### 3.3. Irradiance dependence of the fill factor

The fill factor is a quality parameter of the junction and has a strong influence on the efficiency of a cell. As shown in Fig. 1c, the three cells have a comparable  $FF$  ( $\approx 75\%$ ) under STC. For irradiances between 100 and  $10 \text{ mW}/\text{cm}^2$ , the  $FF$  remains almost constant for the two cells with a larger value of  $R_p$ , while it slowly decreases for the cr cell. When moving towards lower intensities, the  $FF$  of this cell abruptly decreases. The decrease is less sharp for the std cell and even less for the copper poor one, which retains a value of the  $FF$  of approximately 60% at  $0.1 \text{ mW}/\text{cm}^2$ . Table 2 summarises the values of the cell parameters measured at  $0.1 \text{ mW}/\text{cm}^2$  and shows how, under this illumination intensity, a larger  $R_p$  of the cell clearly corresponds to higher values of  $V_{OC}$ ,  $FF$ , and, therefore of  $\eta$ .

Table 2

Photovoltaic parameters of the three cells with different Cu contents measured at  $0.1 \text{ mW/cm}^2$  ( $10^{-3}$  sun). At this irradiance value, a larger  $R_p$  clearly corresponds to higher values of open-circuit voltage  $V_{OC}$ , fill factor  $FF$ , and, therefore of the efficiency  $\eta$

Sample name	Irradiance: $0.1 \text{ mW/cm}^2$ Cu content [at.%]	$R_p$ ( $\text{k}\Omega \text{ cm}^2$ )	$FF$ (%)	$V_{OC}$ (mV)	$I_{sc}$ ( $\mu\text{A/cm}^2$ )	$\eta$ (%)
cr	23.3	3.5	25.4	93.9	27.8	0.7
std	21.5	11.8	31.6	256	25.4	2.3
cp	18	142	57.1	405	23.6	6

### 3.4. Structure and morphology of $\text{Cu(In,Ga)Se}_2$ films

Fig. 2 presents SEM images of the cross-section of the three samples. It is well known that the amount of Cu in the absorber material strongly influences the morphology and structure of the film [7]. The main effect of reducing the Cu content in the film is that of modifying the shape and reducing the size of the film grains. The cr film clearly shows an ordered columnar growth of the grains which have a size of approximately  $2\text{--}4 \mu\text{m}$ , perpendicular to the back contact Mo-surface. The film morphology of the std film does not vary

(oriented columnar growth of the grains) but the grain size is clearly smaller ( $1\text{--}1.5 \mu\text{m}$ ). In the cp film there is no longer a preferred growth orientation and the columnar-like shape of the grains is interrupted by the presence of horizontal grain boundaries. The number of grains directly connecting the back to the front contact is, therefore strongly reduced, and the grain sizes ( $\approx 0.5 \mu\text{m}$ ) as well.

### 3.5. Resistivity measurements on $\text{Cu(In,Ga)Se}_2$ films

The bulk resistivity  $\rho$  of the samples characterised in the first part of the work, as well as of other samples, was measured using a coplanar contact geometry. The film with the higher Cu content (23.3 at.%) has a  $\rho$  of  $12 \Omega\text{cm}$ . This parameter increases when reducing the Cu content of the film (see Fig. 3) up to a value of  $\rho = 115 \Omega\text{cm}$  for the Cu-poor film (Cu content: 18 at.%). Since the cross-grain conductivity in a polycrystalline film is determined by the grain boundaries, this behaviour is explained by considering the SEM images presented above. The lowering of the Cu content in the film results in a reduced size of the grains and therefore in an increase of the grain boundary density which lowers the film conductivity.

Fig. 3 also presents the value of  $R_p$  (measured in the dark) plotted as a function of the Cu content of the cells realised with the corresponding absorber materials.  $R_p$

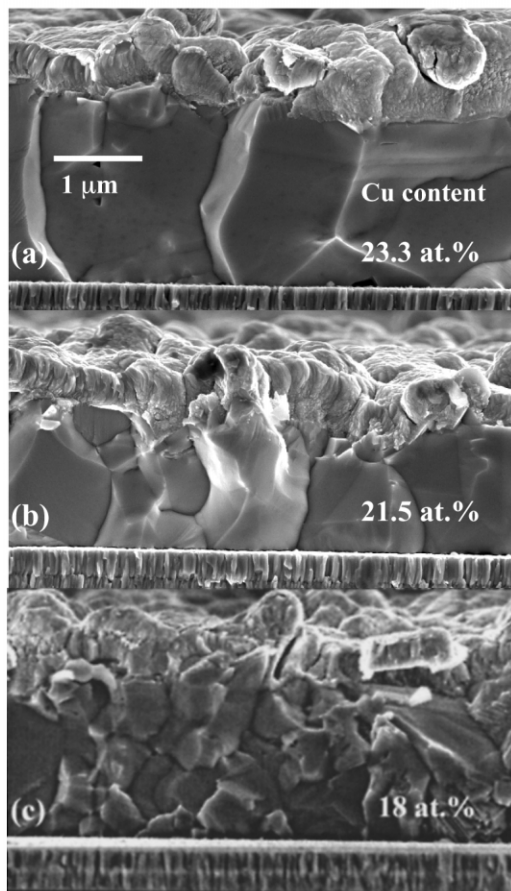


Fig. 2. Scanning electron micrograph images of the cross section of the three cells with different Cu contents (from top to bottom 23.3, 21.5 and 18 at.%).  $\text{Cu(In,Ga)Se}_2$  films are grown on Mo and covered by the  $\text{CdS/ZnO}$  buffer-window system.

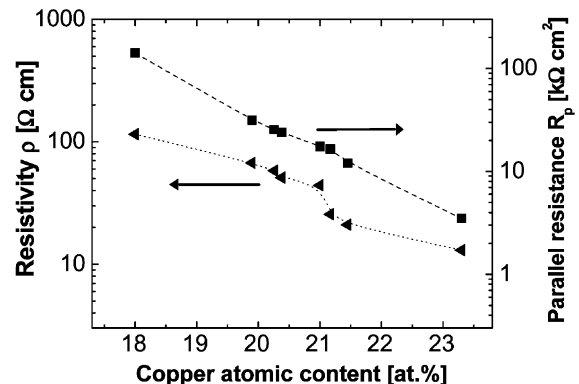


Fig. 3. Resistivity  $\rho$  of  $\text{Cu(In,Ga)Se}_2$  films and parallel resistance  $R_p$  (dark measurement) of the cells plotted as a function of the corresponding Cu content in the absorber film. Lines are included as guides to the eye.

increases from 3.5 k $\Omega$  cm<sup>2</sup> to 142 k $\Omega$  cm<sup>2</sup> when moving from the most Cu-rich to the most Cu-poor sample. We therefore observe that the shunting behaviour of a cell is directly proportional to the resistivity  $\rho$  of its absorber material.

#### 4. Discussion—Nature of the parallel resistance in Cu(In,Ga)Se<sub>2</sub> cells

The parallel resistance  $R_p$  of a solar cell often has a macroscopic origin, in the sense that it arises from edge effects or highly localised pinholes. The devices investigated in this work were carefully chosen in such a way as to avoid the presence of such macroscopically localised defects. For these devices, we have shown that  $R_p$  is dominated by the choice of the absorber material and increases by two orders of magnitude when moving from the most Cu-rich to the most Cu-poor Cu(In,Ga)Se<sub>2</sub>. Furthermore,  $R_p$  of the solar cells is proportional to the resistivity  $\rho$  of the corresponding absorber material. If this proportionality is more than mere coincidence, it should contain a hint towards the intrinsic origin of shunting in Cu(In,Ga)Se<sub>2</sub> solar cells. We will discuss two possibilities below

1. Grain boundaries in polycrystalline thin-film absorbers are a likely origin of shunt paths. If the grain boundaries are type-inverted, they could directly connect the n-type buffer to the metallic back contact. While a higher density and, presumably, a larger activity of grain boundaries would explain the observed decrease of the film conductivity with decreasing Cu-content in the material, the same considerations would also predict a lower shunt resistance for the corresponding devices, i.e. a trend that is just opposite to the experimental observation. The grain boundary hypothesis only makes sense in a modified form. Let us assume that only a small part  $p$  of the grain boundaries, e.g. because of their special crystallographic nature, can carry a considerable shunt current. Because of the columnar structure of the grains in the more Cu-rich films, the parallel conductance would be directly proportional to  $p$ . The random nature of grain boundaries in the small-grained Cu-poor material does not allow a direct connection of the front and back contacts by one single grain boundary. The probability to find, say three, highly conducting grain boundaries directly connected to each other would then be proportional to  $p^3$ , i.e. the parallel conductivity could be easily several orders of magnitude smaller than in large-grained material, even though the sheer number of grain boundaries is much larger in the small grained (Cu-poorer) material. Although, this ‘percolation hypothesis’ might explain our experimental results, it relies on relatively special assumptions on grain boundary properties and

there might be a more natural explanation for our results.

2. A more straightforward model to explain our experimental results assumes the presence of highly localised regions in the material that provide a high recombination current density. We may think of these ‘hot spots’ in terms of nano-scale phase segregations in the space charge region of the absorber or localised damage at the absorber–buffer interface. If these regions are small enough to be embedded in a matrix of regular absorber material, the shunt current carried by the hot spots is always limited by the spreading resistance of the embedding absorber material. This idea would provide a natural connection between the bulk resistivity of the absorber material and the shunt resistance of the corresponding device. The spreading resistance  $R_{sp}$  of a sphere with radius  $r$  embedded in a matrix material with resistivity  $\rho$  is  $R_{sp} = \rho/(\pi r)$ . Assuming that the resistance of such a high recombination volume is small compared to the spreading resistance yields the proportionality

$$R_p = \rho/nr\pi \quad (4)$$

for a density  $n$  of those hot spots per unit cell area. Thus, e.g.  $n = 10^8$  cm<sup>-2</sup> with  $r = 3$  nm or  $n = 10^7$  cm<sup>-2</sup> with  $r = 30$  nm would explain the observed relationship  $R_p/\rho \approx 10^{-4}$  cm between the parallel resistance  $R_p$  of the solar cell and the absorber resistivity  $\rho$ . The volume fraction  $f_v$  of the high-recombination sites would then be  $f_v = \pi nr^3/d \approx 10^{-7}$  or  $10^{-5}$  in a film of thickness  $d = 1$   $\mu$ m for  $r = 3$  nm or  $r = 30$  nm, respectively.

In view of the simplicity of its arguments we favour the second hypothesis, though more microscopic investigations are required to find a conclusive answer.

#### 5. Conclusions

We present a Cu(In,Ga)Se<sub>2</sub> cell whose low-irradiance performance is notably increased. In the typical indoor-irradiance range (0.05–5 mW/cm<sup>2</sup>), the efficiency  $\eta$  of the cell varies between 5 and 10.5% and the open circuit voltage  $V_{OC}$  between 375 mV and 540 mV. The cell was realised with a highly resistive, copper-poor absorber material (cp-Cu(In,Ga)Se<sub>2</sub>) and exhibited a value of the shunt resistance  $R_p$  which is increased by more than one order of magnitude compared to standard Cu(In,Ga)Se<sub>2</sub> cells. Moreover, we note that the bulk resistivity of the absorber material is directly proportional to the  $R_p$  of the corresponding solar cell and try to give a description of the physical nature of this parameter, focusing our attention on two possibilities: 1) the effect of grain boundaries; 2) the presence of highly localised regions of high recombination embedded in a matrix of regular absorber material.

## Acknowledgments

We gratefully acknowledge the ZSW and Würth Solar CIS teams for support and especially Christine Ochotzki for the SEM images. This work was supported by the ‘Bundesministerium fuer Bildung und Foscung’ (BMBF) under contract 16V1121/0.

## References

- [1] D.L. Bätzner, A. Romeo, H. Zogg, A.N. Tiwari, in: B. McNelis, W. Palz, H.A. Ossenbrinck, P. Helm, (Eds.), Proceedings of the 17th European Photovoltaic Solar Energy Conference, WIP-Munich, Germany, 2002, 1180.
- [2] J.F. Randall, C. Droz, M. Goetz, A. Shah, J. Jacot, in: B. McNelis, W. Palz, H. A. Ossenbrinck, P. Helm (Eds.) Proceedings of 17th European Photovoltaic Solar Energy Conference, WIP-Munich, Germany, 2002, 603.
- [3] A. Virtuani, E. Lotter, M. Powalla, *Thin Solid Films* 431–432 (2003) 443.
- [4] M. Powalla, M. Cemernjak, A. Eicke, J. Springer, A. Sorg, U. Stein, G. Voorwinden, A. Zeller, B. Dimmler, in: H. Scheer, B. McNelis, W. Palz, H. A. Ossenbrink, P. Helm (Eds.) Proceedings of the 16th European Photovoltaic Solar Energy Conference, James and James, London, 2000, p. 275.
- [5] R. Klenk, T. Walter, H.W. Schock, D. Cahen, *Adv. Mater.* 5 (1993) 114.
- [6] [www.diplot.de](http://www.diplot.de).
- [7] J.R. Tuttle, D.S. Albin, R. Noufi, *Solar Cells* 30 (1991) 21.